5-13-2016

Towards Bipedal Behavior on a Quadrupedal Platform Using Optimal Control

Turner Topping
University of Pennsylvania, ttopping@seas.upenn.edu

Vasileios Vasilopoulos
University of Pennsylvania, vvasilo@seas.upenn.edu

Avik De
University of Pennsylvania, avik@seas.upenn.edu

Daniel E. Koditschek
University of Pennsylvania, kod@seas.upenn.edu

Towards Bipedal Behavior on a Quadrupedal Platform Using Optimal Control

Abstract
This paper explores the applicability of a Linear Quadratic Regulator (LQR) controller design to the problem of bipedal stance on the Minitaur [1] quadrupedal robot. Restricted to the sagittal plane, this behavior exposes a three degree of freedom (DOF) double inverted pendulum with extensible length that can be projected onto the familiar underactuated revolute-revolute "Acrobot" model by assuming a locked prismatic DOF, and a pinned toe. While previous work has documented the successful use of local LQR control to stabilize a physical Acrobot, simulations reveal that a design very similar to those discussed in the past literature cannot achieve an empirically viable controller for our physical plant. Experiments with a series of increasingly close physical facsimiles leading to the actual Minitaur platform itself corroborate and underscore the physical Minitaur platform corroborate and underscore the implications of the simulation study. We conclude that local LQR-based linearized controller designs are too fragile to stabilize the physical Minitaur platform around its vertically erect equilibrium and end with a brief assessment of a variety of more sophisticated nonlinear control approaches whose pursuit is now in progress.

Disciplines
Electrical and Computer Engineering | Engineering | Systems Engineering

Towards Bipedal Behavior on a Quadrupedal Platform Using Optimal Control

T. Turner Topping[a], Vasileios Vasilopoulos[b], Avik De[a], and Daniel E. Koditschek[a]

[a]Electrical & Systems Engineering, University of Pennsylvania, Philadelphia, PA
[b]Mechanical Engineering and Applied Mechanics, University of Pennsylvania, Philadelphia, PA

ABSTRACT

This paper explores the applicability of a Linear Quadratic Regulator (LQR) controller design to the problem of bipedal stance on the Minitaur [1] quadrupedal robot. Balancing the body on only the rear legs affords the possibility of using the front legs for other tasks such as manipulation or bracing. Restricted to the sagittal plane, this behavior exposes a 3DOF (degree of freedom) double inverted pendulum with extensible length actuated at the prismatic ("shank") and second revolute ("knee/hip") joints per Figure 1 and section 2.1. Locking the prismatic (shank) DOF reduces the Lagrangian model of the pinned toe mechanism to that of the familiar singularly-actuated 2 DOF (revolute-revolute) acrobot per section 2.2 and lemma 2.1 . Since the linearized 3DOF dynamics at any vertically erect stance exposes a decoupled linearized acrobot, we focus on stabilizing this subsystem in isolation per section 2.3.

Previous work has documented the empirical stabilization of a physical acrobot using a local LQR controller[2,3]. However, MATLAB simulations reveal that an LQR design very similar to those discussed in the past literature cannot achieve an empirically viable controller for our physical plant. First, the design is not robust, failing to stabilize the Minitaur model in numerical simulations run with a variety of small inaccuracies in presumed kinematic and dynamic parameters (none greater than than 5% of the putative value), even when the system starts at rest nearly exactly in the desired erect vertical equilibrium state per section 3.1.1 and tables 1 and 2. The fragility of the LQR design is similarly manifest when run on the Minitaur platform model whose initial prismatic shank extension length differs by an amount less 0.4% of its full range, and with initial body and leg angle conditions whose deviation relative to the desired erect vertical equilibrium goal state also lies beneath the sensor resolution threshold, per 3.1.2, fig. 2. Even worse, the acrobot physically instantiated by locking the actual Minitaur's leg extension has an (unactuated) stance toe angle lacking a joint sensor so that its (intertial frame) body orientation must actually be inferred from IMU-driven estimators whose resolution (in both space and time) is considerably worse than that of its available (actuated) joint sensors (whereas the joint encoders offer 9 bits of useful resolution, the IMU position estimates have a noise floor of $\pm 3^\circ$-just under 1% of their 360° range) per 3.1.3, and figs 4, 3. Experimental studies using derivative measurments from the filtered IMU output show that the commensurately lagging joint velocity filter time constants cannot support the derivative gains required by the LQR design (per footnote †). Suitably lowered derivative gain magnitudes found by ad hoc tuning * resulted in successful stabilization of the numerical acrobot model with physically realizable sensor estimation and actuator gains per section 3.1.4 and fig. 5. Unfortunately, further numerical study of the nonlinear Acrobot model revealed that the basin of attraction around the vertically erect equilibrium afforded by these physically realizable gains lay nearly below the physical (IMU-driven) sensor noise floor.

This paper reports on experiments with two different approximate variants of the physical Minitaur platform that corroborate and underscore the implications of the simulation study. On a physical instance of the literal Acrobot scaled to minitaur proportions, equipped with high resolution (9-bit) joint sensors at both revolute (toe and hip/knee) joints, we successfully implemented both the local LQR design as well as its ad hoc relaxation

Further author information: (Send correspondence to T.T. Topping.)
T.T.Topping: E-mail: ttopping@seas.upenn.edu
V. Vasilopoulos.: E-mail: vvasilo@seas.upenn.edu

* Lowered-gains magnitudes can of course be achieved by ad hoc adjustment of the LQR cost structure, but our repeated efforts along these lines led to controllers whose sensitivity to parametric error was an order of magnitude worse than reported above.

(with diminished velocity gains) - albeit the latter only from initial conditions extraordinarily carefully placed at the targeted physically erect equilibrium state 3.2.1, fig. 9. We then attempted to run the same experiments on a second variant: a literal Minitaur platform that we modified by pinning its toes along a fixed axis, thereby forming a literal revolute first joint. † As predicted by our numerical study, neither the original LQR design, nor its velocity-gain relaxation succeeded in stabilizing the toe-pinned but IMU-driven Minitaur's vertically erect equilibrium state per section 3.2.2 and figure 10. Finally, for completeness, an unmodified Minitaur model was tested to confirm the failure of the LQR based controller for bipedal stance 3.2.3, fig 11.

We conclude that local LQR-based linearized controller designs are too fragile to stabilize the physical Minitaur platform around its vertically erect equilibrium and end with a brief assessment of a variety of more sophisticated nonlinear control approaches whose pursuit represents work presently in progress.

Keywords: Nonlinear Control, LQR, Bipedal Stance, Legged Robots

1. INTRODUCTION

This paper documents experiments and simulation pertaining to achieving bipedal stance with a quadrupedal platform using a Double Inverted Pendulum (DIP) model and a Linear Quadratic Regulator (LQR) controller. Due to sensor resolution constraints as well as assumptions about the physical system implicit in the DIP model that do not hold, achieving bipedal stance using such a controller and model is impossible.

Bipedal robots have been an emphasized area of robotics research for some time [4,5,6]. While many of these bipedal platforms have had high numbers of degrees of freedom and move slowly, more dynamic bipeds like Marc Raibert's[7], or the ATRIAS[8] have demonstrated a fundamentally different approach to bipedal locomotion. Furthermore, research on bipedal locomotion with a hexapod platform [9] has shown the promising prospect of using this approach on platforms like Minitaur, which would allow for a rich family of behaviors to be implemented that are otherwise unattainable in quadrupedal stance without the help of another actuator. Such behaviors could allow the Minitaur platform to achieve otherwise impossible tasks like reaching for objects higher than a body length and manipulating them, or reaching and operating a door handle, a task that is difficult even with much more expensive and complex systems, as was shown in the DARPA Robotics Challenge. This paper further shows the necessity for dynamical control schemes for bipedalism on Minitaur, for while physical DIPs like the Acrobot have been controlled sufficiently well by optimal control methods like LQR [2,3], and while the DIP has been used as a model for bipedal stance in robotics [10], such methods will fail on the Minitaur platform due to the fragility of LQR control.

2. THEORY

During bipedal standing, Minitaur can be approximated as a 3DOF (degree of freedom) double inverted pendulum in the sagittal plane, as shown in Fig. 1, where the two hind legs act in parallel as a virtual monoped and are equivalent to the first link of the kinematic chain. Note that each leg actually physically consists of two pairs of rigid links with length L_1 and L_2. Hence, the first DOF corresponds to the body pitch angle with respect to the horizontal, φ, while the other two DOF are the angles θ_1 and θ_2 of each leg link with length L_1 with respect to the body. It must be noted that θ_1 and θ_2 are actuated and correspond to the two DOF of the leg 5-bar mechanism, as described in [1].

† Notice that the Acrobot model presumes a pinned revolute first joint whereas Minitaur's physical toe will lift off whenever its ground reaction force vector exhibits a nonpositive normal component. While both the original LQR and relaxed feedback structures yield simulated acrobot motions that typically do not violate these constraints within their respective basins of attraction, the unstable motions resulting from basin violations inevitably do so per section 3.1.4 specifically figure 7. Physically pinning the Minitaur's toes eliminated this potentially confounding departure from the assumptions underlying the acrobot linearized controller designs.

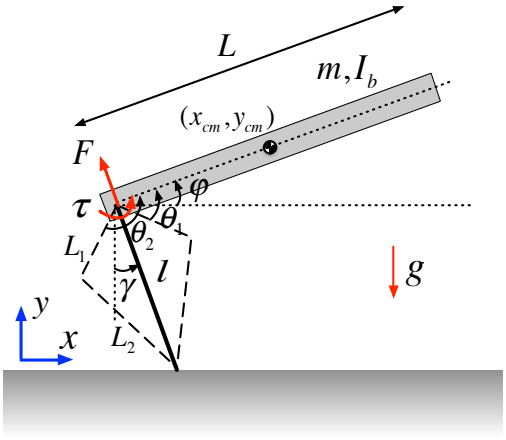

Figure 1. Model of the robot in the sagittal plane.

2.1 Kinematics

Instead of directly dealing with θ_1 and θ_2, a more intuitive approach of describing the leg length and angular position with respect to the vertical passing through the hip, using two equivalent variables l and γ respectively, can be adopted. Using simple geometric relations, the first link of the kinematic chain in the double inverted pendulum model can be expressed as:

$$l = L_1 \cos\left(\frac{\theta_2 - \theta_1}{2}\right) + \sqrt{L_2^2 - L_1^2 \sin^2\left(\frac{\theta_2 - \theta_1}{2}\right)} \tag{1}$$

$$\gamma = \pi - \frac{\theta_1 + \theta_2}{2} + \varphi \tag{2}$$

In this way, a triplet $(\theta_1, \theta_2, \varphi)$ can be always corresponded to a triplet (l, γ, φ). On the other hand, if l, γ and φ are known, θ_1 and θ_2 can be found using the following equations

$$\theta_1 = \pi/2 - (\gamma - \varphi) - \cos^{-1}\left(\frac{l^2 + L_1^2 - L_2^2}{2L_1 l}\right) \tag{3}$$

$$\theta_2 = \pi/2 - (\gamma - \varphi) + \cos^{-1}\left(\frac{l^2 + L_1^2 - L_2^2}{2L_1 l}\right) \tag{4}$$

which are similar to the kinematic relations presented in [11]. Hence, instead of τ_1, τ_2, that directly act on θ_1 and θ_2 respectively, we can use the inverse kinematics and define two new virtual inputs τ and F, as shown in Fig. 1, which act on the relative angle $\beta = \gamma - \varphi$ and l respectively, as follows

$$\tau := -\frac{\partial \theta_1}{\partial \beta}\tau_1 - \frac{\partial \theta_2}{\partial \beta}\tau_2 \tag{5}$$

$$F := -\frac{\partial \theta_1}{\partial l}\tau_1 - \frac{\partial \theta_2}{\partial l}\tau_2 \tag{6}$$

Note that the signs in the equations above are chosen for compliance with the positive notation for the torques. In this way, the system dynamics can be now extracted using l, γ and φ as degrees of freedom and τ, F as the inputs.

2.2 Dynamical Analysis & Reduction to Acrobot

For the dynamical analysis that follows, the following assumptions were made:

- The leg mass and inertia are significantly smaller than those of the main body and can be neglected. This assumption actually corresponds to reality since each Minitaur leg weighs approximately 150g, which is significantly smaller than the main body mass (approximately 5kg).
- The body COM (center of mass) is located at the middle of the body.
- The leg toe never leaves the ground. This assumption must hold when the robot exhibits the desired behavior, since the robot is not allowed to jump. Because this assumption was later violated, experiments were performed where the toe was pinned, making it a physical revolute joint. A more extensive discussion on this issue will be performed in the following sections.

Under these assumptions, the system's kinetic energy can be expressed as

$$T = \frac{1}{2}m\left[(\dot{x}_{cm})^2 + (\dot{y}_{cm})^2\right] + \frac{1}{2}I_b\,\dot{\varphi}^2 \tag{7}$$

where m and I_b are the body mass and body inertia respectively, while the potential energy can be expressed as

$$U = mg\,y_{cm} \tag{8}$$

In the equations above, (x_{cm}, y_{cm}) denotes the position of the body COM in absolute coordinates in the sagittal plane, as shown in Fig. 1 and given by

$$x_{cm} = -l\sin\gamma + 0.5L\cos\varphi \tag{9}$$

$$y_{cm} = l\cos\gamma + 0.5L\sin\varphi \tag{10}$$

where L is the length of the main body (hip to hip).

In this way, the Lagrangian of the system is defined as

$$\mathcal{L} = T - U = \frac{1}{2}m\left[(\dot{x}_{cm})^2 + (\dot{y}_{cm})^2\right] + \frac{1}{2}I_b\,\dot{\varphi}^2 - mg\,y_{cm} \tag{11}$$

Finally, the power input to the system is written as

$$P_t = \tau(\dot{\gamma} - \dot{\varphi}) + F\dot{l} \tag{12}$$

Each one of the three second-order differential equations of motion can be then written out by expanding the Euler-Lagrange operator for each one of the variables l, γ and φ as follows

$$\frac{d}{dt}\left(\frac{\partial\mathcal{L}}{\partial\dot{\alpha}}\right) - \frac{\partial\mathcal{L}}{\partial\alpha} = \frac{\partial P_t}{\partial\dot{\alpha}} \quad \text{for} \quad \alpha = l, \gamma, \varphi \tag{13}$$

Therefore, we get the following equations:

$$m\ddot{l} + 0.5mL\cos(\gamma-\varphi)\ddot{\varphi} - ml\dot{\gamma}^2 + 0.5mL\sin(\gamma-\varphi)\dot{\varphi}^2 + mg\cos\gamma = F \tag{14}$$

$$ml^2\ddot{\gamma} - 0.5mLl\sin(\gamma-\varphi)\ddot{\varphi} + 2ml\dot{l}\dot{\gamma} + 0.5mLl\cos(\gamma-\varphi)\dot{\varphi}^2 - mlg\sin\gamma = \tau \tag{15}$$

$$0.5mL\cos(\gamma-\varphi)\ddot{l} - 0.5mLl\sin(\gamma-\varphi)\ddot{\gamma} + (I_b + 0.25mL^2)\ddot{\varphi} - 0.5mLl\cos(\gamma-\varphi)\dot{\gamma}^2 - mL\dot{l}\sin(\gamma-\varphi)\dot{\gamma} + 0.5mLg\cos\varphi = -\tau \tag{16}$$

It is also interesting to compare the 3DOF dynamical structure of the system developed here to the most common and used in the literature acrobot [12]. Intuitively, we could suggest that the actual 3DOF system could be corresponded to the acrobot by fixing the leg extension l at a specific value. Thus, we are led to the following lemma:

LEMMA 2.1. *If $\dot{l}(t) \equiv 0, \forall t \geq 0$, then the 3DOF double inverted pendulum is reduced to a 2DOF acrobot, whose first link has length $r = l(0)$.*

Proof. By differentiating (9) and (10), we get

$$\dot{x}_{cm} = -\dot{l}\sin\gamma - l\dot{\gamma}\cos\gamma - 0.5L\dot{\varphi}\sin\varphi \tag{17}$$

$$\dot{y}_{cm} = \dot{l}\cos\gamma - l\dot{\gamma}\sin\gamma + 0.5L\dot{\varphi}\cos\varphi \tag{18}$$

Assume that $\dot{l}(t) \equiv 0, \forall t \geq 0$. This means that $l(t) = l(0) = r = \text{const.}, \forall t \geq 0$. Since l remains constant throughout the motion, the system is deprived of its first degree of freedom and its configuration can be uniquely determined by γ and φ. Hence, (17) and (18) are now written as

$$\dot{x}_{cm} = -r\dot{\gamma}\cos\gamma - 0.5L\dot{\varphi}\sin\varphi \tag{19}$$

$$\dot{y}_{cm} = -r\dot{\gamma}\sin\gamma + 0.5L\dot{\varphi}\cos\varphi \tag{20}$$

Finally, from (12), for $\dot{l} \equiv 0$ we get the power input

$$P = \tau(\dot{\gamma} - \dot{\varphi}) \tag{21}$$

which shows that the force F is eliminated and the torque τ is the only remaining input.

Assuming now an acrobot, with a first, massless link of fixed length r and a second link identical to the body of the 3DOF system as shown in Fig. 1, described by the same two DOF (namely γ and ϕ) and having only one input (hip torque τ), the position (x_{acr}, y_{acr}) of its center of mass in the sagittal plane would be

$$x_{acr} = -r\sin\gamma + 0.5L\cos\varphi \tag{22}$$

$$y_{acr} = r\cos\gamma + 0.5L\sin\varphi \tag{23}$$

so that

$$\dot{x}_{acr} = -r\dot{\gamma}\cos\gamma - 0.5L\dot{\varphi}\sin\varphi \tag{24}$$

$$\dot{y}_{acr} = -r\dot{\gamma}\sin\gamma + 0.5L\dot{\varphi}\cos\varphi \tag{25}$$

It can be seen that (24) is identical to (19) and (25) is identical to (20). This suggests that the Lagrangian $\mathcal{L}_{acr}$ of the acrobot will be identical to the Lagrangian $\mathcal{L}$ of the 3DOF system, since both the kinetic energy and the potential energy of the two systems are identical. Also, for the acrobot system the power input P_{acr} is given by

$$P_{acr} = \tau(\dot{\gamma} - \dot{\varphi}) \tag{26}$$

which is identical to (21). Since $\mathcal{L}_{acr} = \mathcal{L}$, $P_{acr} = P$ and both systems use the same degrees of freedom, we deduce that their equations of motion are exactly the same and this concludes the proof. □

2.3 Linearized dynamics

Since the ultimate goal is to stabilize the robot in the upright position where $l = \delta = \text{const.}$, $\gamma = 0$ and $\varphi = \frac{\pi}{2}$, it is useful to consider the linearized dynamics around this point. By defining the state variables $x_1 = l$, $x_2 = \gamma$, $x_3 = \varphi$, $x_4 = \dot{l}$, $x_5 = \dot{\gamma}$ and $x_6 = \dot{\varphi}$, we can write the linearized equations of motion about the equilibrium point as

$$\dot{\tilde{x}} = A\tilde{x} + B\tilde{u} \tag{27}$$

where

$$\tilde{x} = \begin{bmatrix} \tilde{x_1} \\ \tilde{x_2} \\ \tilde{x_3} \\ \tilde{x_4} \\ \tilde{x_5} \\ \tilde{x_6} \end{bmatrix} = \begin{bmatrix} x_1 - \delta \\ x_2 \\ x_3 - \frac{\pi}{2} \\ x_4 \\ x_5 \\ x_6 \end{bmatrix} \qquad \text{and} \qquad \tilde{u} = \begin{bmatrix} \tilde{F} \\ \tilde{\tau} \end{bmatrix} = \begin{bmatrix} F - mg \\ \tau \end{bmatrix} \tag{28}$$

and the matrices A, B are given by

$$A = \begin{bmatrix} 0 & 0 & 0 & 1 & 0 & 0 \\ 0 & 0 & 0 & 0 & 1 & 0 \\ 0 & 0 & 0 & 0 & 0 & 1 \\ 0 & 0 & 0 & 0 & 0 & 0 \\ 0 & \frac{I_b g + 0.25 m g L^2}{I_b \delta} & \frac{-0.25 m g L^2}{I_b \delta} & 0 & 0 & 0 \\ 0 & -\frac{0.5 m g L}{I_b} & \frac{0.5 m g L}{I_b} & 0 & 0 & 0 \end{bmatrix} \tag{29}$$

$$B = \begin{bmatrix} 0 & 0 \\ 0 & 0 \\ 0 & 0 \\ \frac{1}{m} & 0 \\ 0 & \frac{I_b + 0.5 m L \delta + 0.25 m L^2}{I_b m \delta^2} \\ 0 & -\frac{\delta + 0.5 L}{I_b \delta} \end{bmatrix} \tag{30}$$

The matrices A and B will be used later for the calculation of the Linear Quadratic Regulator (LQR) controller gains that is used in our work.

3. METHODS & RESULTS

3.1 Simulation and Modeling

3.1.1 Simulation Results With Parameter Value Errors

The mass of the robot greatly affects the system's ability to achieve stance, as the LQR controller achieves the specified lower link length by applying a constant radial force proportional to the robot's estimated mass. Examining simulation trials run with small errors in mass estimation of the system makes it apparent that parameter errors in mass less than 5% greatly restrict the set of intitial conditions from which the system will converge to a stable, upright stance, and mass parameter error greater than that prevent the system from converging at all, even when assuming perfect sensor measurements. This prevents Minitaur from having any useful modifications that might change its mass in a measureable way, without re-measuring and recalculating the controller for each specific use. The following tables show the initial conditions with the largest error in γ and ϕ (from 0° and 90° respectively) for which the system will still converge.

Table 1. Largest anecdotally tested initial conditions still within the basin of attraction based on Mass parameter error

Mass Parameter Error	**Initial γ**	**Initial ϕ**
0%	15°	75°
1%	15°	75°
2%	10°	80°
5%	None	None

Another source of parameter error of concern is that of the lower link length. While the link length is adjustable, depending on the quality of construction and geometry of the physical leg links themselves, and

depending on the use of any toe attachments, errors on the order of a cm greatly reduce the set of initial condtions from which the system can converge to upright stance. *

Table 2. Largest anecdotally tested initial conditions still within the basin of attraction based on specific Leg Length parameter Error

Leg Length Parameter Error	**Initial γ**	**Initial ϕ**
0%	15°	75°
1%	15°	75°
3%	12°	78°
5%	5°	85°

Examamining both sources of parameter error, and recognizing that even with perfect or near perfect sensing as in Tab. 1 and in Tab. 2, demonstrates that using this controller is unlikely to be effective without careful measurement and calibration before each attempt to physically implement it.

3.1.2 Simulation Sensitivity to Initial Conditions

Due to the nature of linearizing the nonlinear system around a particular first kinematic link length, the system becomes increasingly sensitive to error in ϕ and γ as the the error in l increases. As a result, the robustness of the system shows great dependence on the ability of the system to aggressively and accurately control l.

Given that the Minitaur platform has limited sensor resolution, the causes and degree of which will be discussed in the following section, we examine the basin of attraction for Minitaur starting within and near the bounds of its sensor resolution. Considering these sensing limitations, four sets of three simulations were run, where each set has the same inital values γ and ϕ with different initial conditions for l for each, chosen to be in progressively greater error relative to the value used to determine the LQR control parameters. Fig. 2 shows the error in the body angle and relative leg angle from the desired vertical stance. In the case where these errors go to zero, we say the system has converged and is stable. In the case where they do not, we say the system does not converge and is unstable. The result is that if the error in l is 1.2mm, which is the limit of the resolution of the sensor, it becomes apparent the formally guaranteed 'basin of attraction' for initial for initial ϕ and γ does not include a ball of radius greater than even 3 degrees, which is about the error in the IMU. This observation already suggests that the LQR control design will fail on our physical system merely in consequence of the position sensing limitations alone.

3.1.3 Sensor Resolution and Noise

A major problem arises when the sensor resolution of the system is examined. The control system relies on the measurements of AS5145B encoders to determine the value of l. The encoder is 12-bit, and the 2-3 least significant bits are lost to noise[13]. This results in a virtually noiseless 9 bit measurement. A quick analysis of the system shows that the worst resolution for the toe position measurement occurs in such a configuration where a change in the θ of the motor and the resulting tangent motion of the far end of the physical upper leg link is parallel to the motion of the toe, as shown in Fig. 3. This configuration limits the resolution of the measurement of l to the shank length, 0.1 meter, multiplied by the angular resolution of the encoder. In this configuration, the system has a l resolution of 0.6mm to 1.2mm.

Similarly, because the system does not enjoy a revolute joint instead of a toe contact, it relies on measurements from an IMU to determine both γ and ϕ. The plot in Fig. 4, shows the error of the IMU estimate of body pitch with respect to the actual body pitch as determined by the motor encoder for motion at a constant 10 Hz. ‡ The resulting RMS value of the error is .0723 radians, more than 4°. As seen in the previous section, the resolution

* While these parameter errors were tested on the 3DOF Minitaur model, the authors verfied that similar reductions in the basin of attraction occur for the 2DOF acrobot model, though not quite as pronounced for mass parameter error

‡The systematic bias observed here is due to the kalman filter drift.

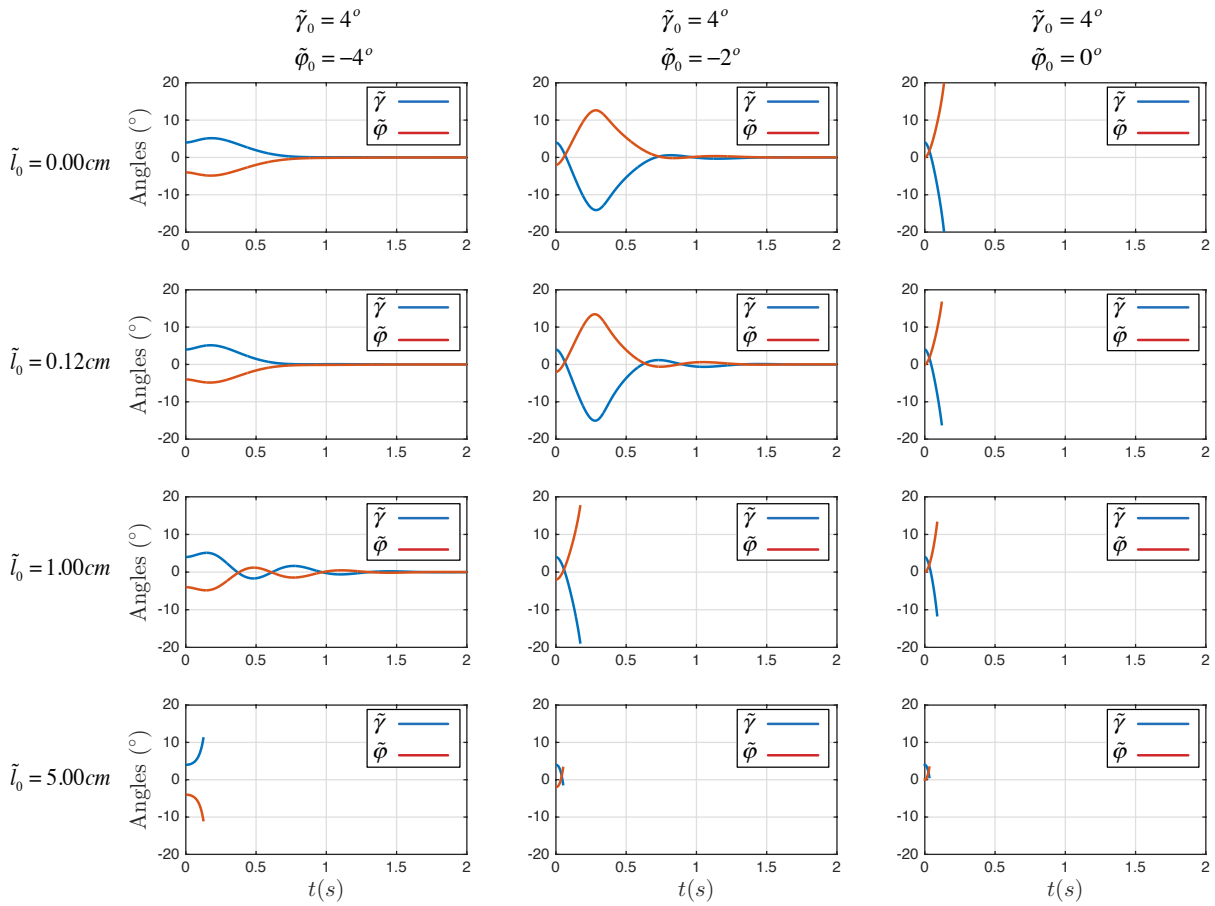

Figure 2. Simulation Results with varying sets of inital conditions for error in ϕ, γ and l which depict stability (when the error ϕ and γ go to zero), and instability (when the error ϕ and γ diverge)

of each of the sensors making starting within the tiny available basin of attraction (+/-3° for l error of 1.2mm) impossible.

In addtion, velocity measurments via the IMU and the encoders are prone to noise due to the differentiation of the encoder signal as well as the IMU velocity error. While the signal is filtered, the bandwidth is fundamentally limited as increased filtering increases delay. Such restrictions prevent the implemenation of the high valued derivative gains required for the LQR controller. Implementing such gains causes an uncontrollable "shaking" which highlights one of the challenges of the minitaur system. Unlike like the Acrobot, which can use encoders at its revolute joints to ascertain accurate measurments of the position and velocities of its links, Minitaur must rely on measurements from an IMU to determine ϕ ,$\dot{\phi}$,γ and $\dot{\gamma}$. The result is that the measurements for $\dot{\phi}$ and $\dot{\gamma}$ are likely much noisier than a measurment from the encoders. When the proportional error is small, even modest derivative gains on $\dot{\gamma}$ and $\dot{\phi}$ will amplify this noise and induce the shaking phenomenon. A liberal upper bound on these derivative gains was empirically determined to be about 10, [†] and references to "reduced LQR gains" will correspond to a set of LQR gains that have reduced derivative terms to comply with this limit.

[†] This was empirically determined by first trying to implement the LQR specified derivative gains, and then finding that without even attempting a trial, the legs would shake uncontrollably. The derivative gains were reduced to zero, and we found that the shaking phenomenon was gone. Then we simply increased the derivative gains as high as we could without reintroducing the shaking phenomenon.

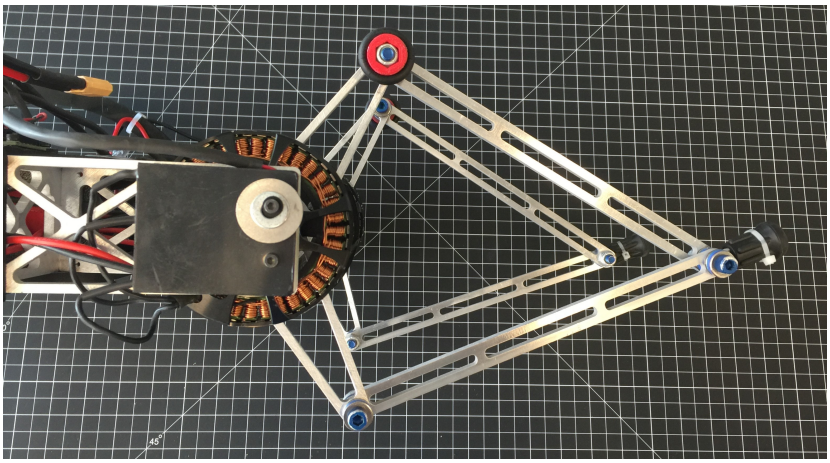

Figure 3. Minitaur Leg in configuration that causes the Lowest Resolution of Toe Extension Position

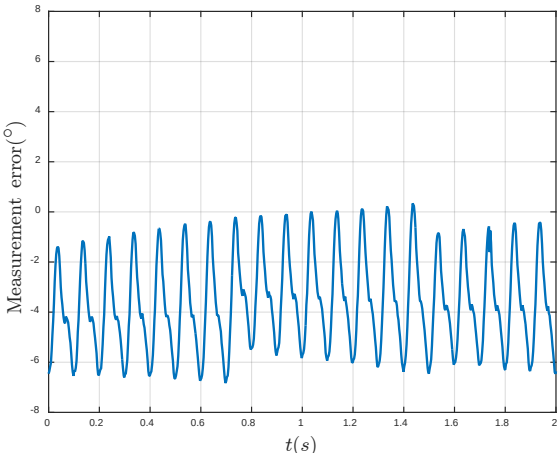

Figure 4. Error of IMU pitch measurement vs body pitch measurements obtained through the AS5145B encoder.

3.1.4 Simulation Results with Ad-Hoc Tuning

As mentioned in section 3.1.3, initial computation of the control system gains gave us high but not unreasonable values for error in $\dot{\phi}$, and $\dot{\gamma}$, which will be reffered to as derivative gains. This set of unreduced gains shows a reasonably large basin of attraction for bipedal standing, and even with reasonably large initial errors in ϕ and θ, the system can converge to its desired pose [‡]. However, imposing the reduced LQR gains on the controller reveals in simulation that, while a basin of attraction exists, per fig. 5, it is much smaller than its unreduced counterpart, as seen in Fig. 6. More concerningly, it is revealed the value of the ground reaction force (GRF) on the toe cross zero in Fig. 7, implying that there is a liftoff, and the model no longer has control authority. This breakdown of the double inverted pendulum model precipitates the "pinning" of the Minitaur platform's toe so as to make it an actual revolute joint, discussed in section 3.2.2.

[‡]These claims are based on the assumption that the intial error in the prismatic extension length is 0

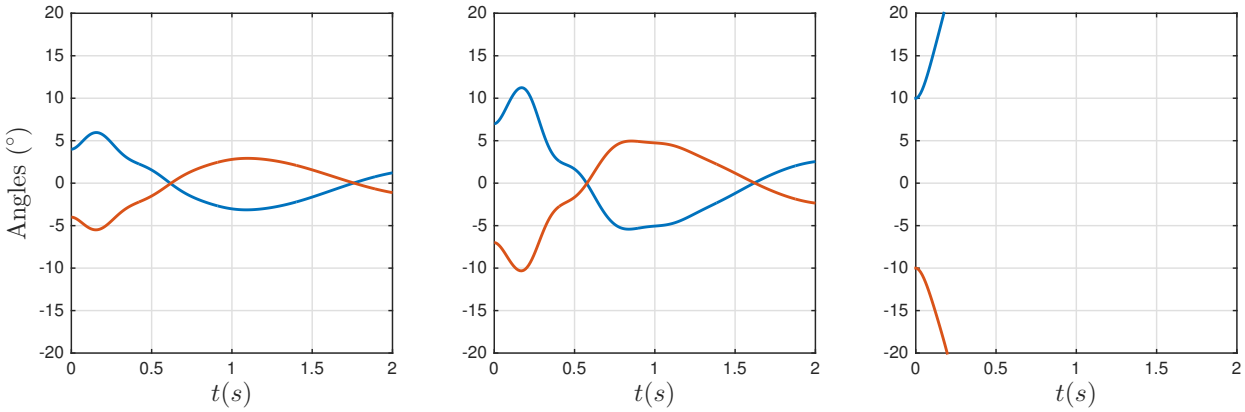

Figure 5. Simulation trials with reduced gains showing the smaller basin of attraction for initial errors ϕ and γ

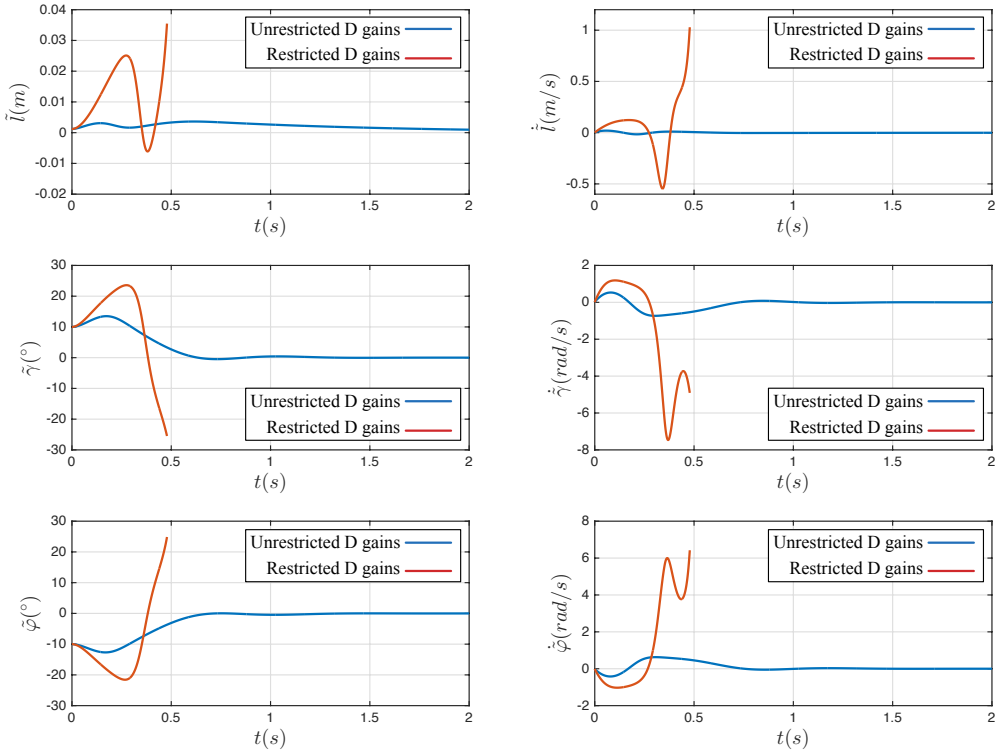

Figure 6. Comparison of simulated trials with LQR gains and reduced gains showing the system's inability to converge in the latter case for the same set of initial conditions

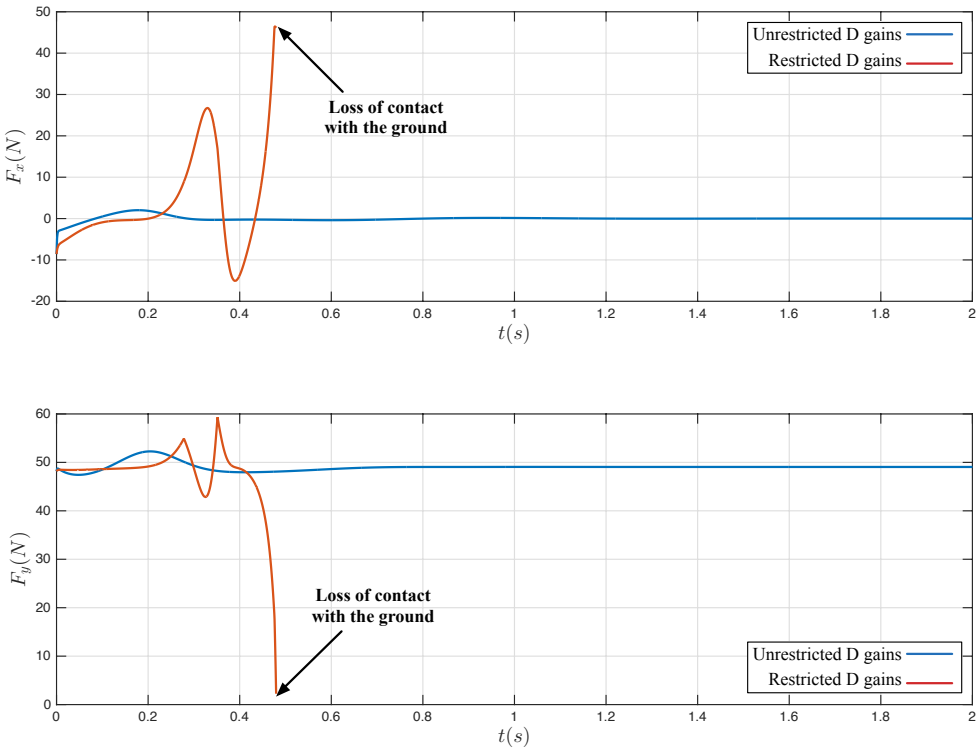

Figure 7. Comparison of ground reaction forces for simulated trials with both the actual and reduced LQR gains, showing that in the latter case their is a liftoff condition

3.2 Robot Experiments

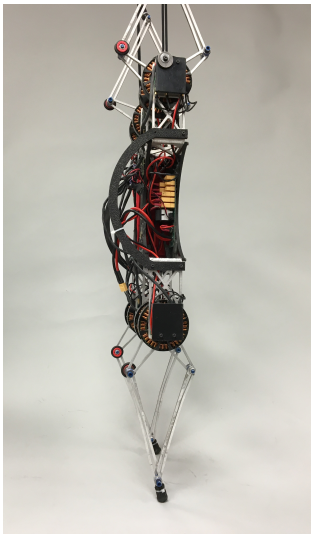

Figure 8. Minitaur at the Beginning of an Experimental Trial

3.2.1 Literal Acrobot Results

To validate our implementation of LQR control methods, experimental trials were performed on a literal acrobot, sharing similar characteristics as the Minitaur platform in terms of body length, and lower link length. The trials

were successful, but convergence requires placing the acrobot very near to the desired vertical position initially. The plot below shows the error in body angle and relative leg angle from the desired vertcal stance of time, which converge from their initial conditions. [§]

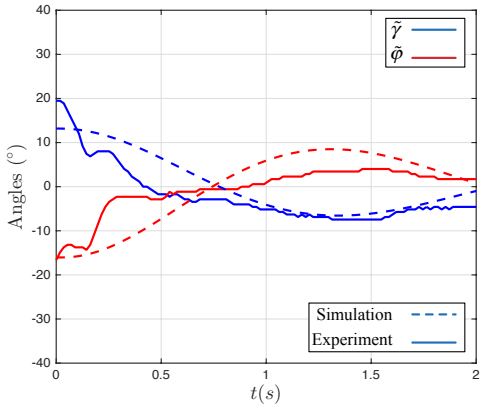

Figure 9. Body pitch and relative leg angle error (ϕ and γ) converging during this literal acrobot trial, compared with simulated trial

3.2.2 Pinned Results

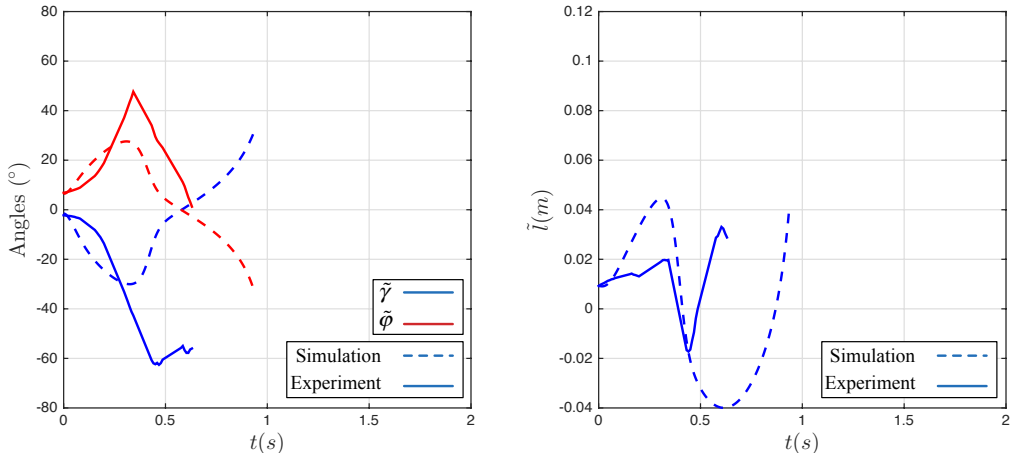

Figure 10. Comparison of the error in γ,ϕ and l for simulated trial and for a trial on Minitaur with a pinned toe, showing a similar failure to converge in both

After succesfully implementing a literal acrobot, we attempted to run the same experiments on a second variant: a literal Minitaur platform that we modified by pinning its toes along a fixed axis, thereby forming a literal revolute first joint. However, even in a simulated trial where the initial leg length error $\tilde{l}$ and $\dot{l}$ were both as near zero as is possible to acheive in experiment and the initial conditions well within a reasonable starting basin of $\phi = 87°$ and $\gamma = 3°$, the model fails to acheieve upright stance. These results were verified in an experimental trial with the same initial condtions. The results of the subsequent experimental and simulated trials, are shown

[§]The plot below shows convergence to about 5 degrees from the vertical position. This is due in part to the lower gains on this acrobot model, as the mass of the upper link is significantly less than that of the Minitaur platform, and thus requires significantly lower magnitude gains, and to the cogging torque and stiction in the physical system.

in Fig. 10, suggest a reasonable agreement between experiment and the simulated model, and thus suggest the experimental attempts are failing for the reasons outlined previously.

3.2.3 Unpinned Results

For completeness, Minitaur was tested without pinned toes with the set of reduced LQR gains. Minitaur was started in a near vertical position, with a leg extension as close to the 20cm equilibrium point as was possible. Fig. 11, show the failure of the system to converge to the desired vertical stance. This result validates the inability of the system to converge to equilibrium starting with initial conditions that were humanly possible to obtain.

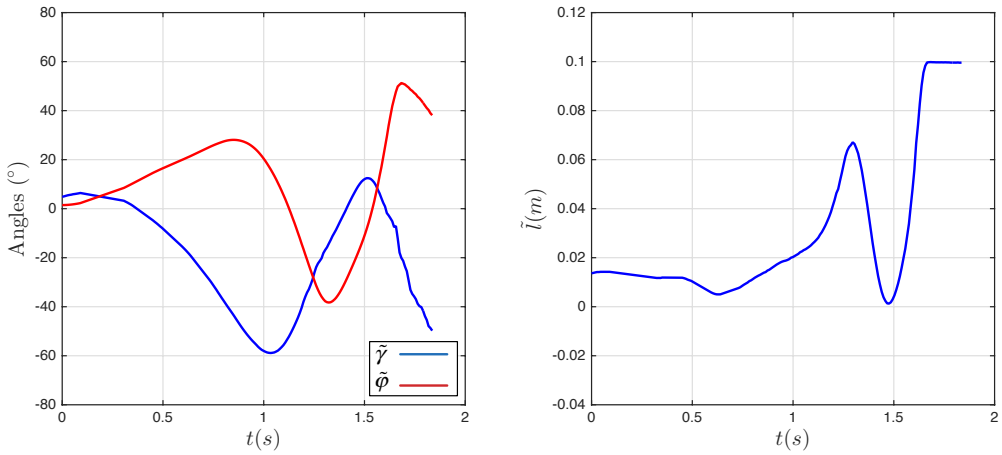

Figure 11. Error in γ,ϕ and l from desired vertical stance for trial with unpinned toe, showing a failure to converge

4. CONCLUSION AND FUTURE WORK

We have demonstrated many aspects of the system and model that make bipedal stance impossible with an LQR controller on Minitaur. While sensor resolution renders this method of control impossible on the current Minitaur platform, given the controller's sensitivities to the first kinematic link length, it is unlikely that even with vastly improved sensors, the controller will ever be effective. Further research wil also be conducted to try and conclude that quasi-static bipedal stance is unachieveable on the Minitaur platform by looking exhaustively at other models and controllers. We believe that looking at dynamic bipedal motion such as two-legged hopping will provide a much more suitable solution to achieving the desired bipedal behaviors.

.1 Optimal Control using LQR

While this paper alludes to the appropriateness of using a modified double inverted pendulum model as the basis for bipedal standing, the specific focus is on the effectiveness of using an LQR controller, as presented in [3], for such a task.

From optimal control theory and for the continuous-time linear time-invariant system shown in (27), we know that we can define a cost functional that must be minimized, as follows

$$J = \int_0^\infty \left(\tilde{x}^T Q \tilde{x} + \tilde{u} R \tilde{u}\right) dt \tag{31}$$

Here, Q is a 6x6 positive-definite matrix representing the state costs and R is a 2x2 positive-matrix representing the input costs. The feedback control law that minimizes the cost functional J is then

$$\tilde{u} = -K\tilde{x} \tag{32}$$

where the gain matrix K is given by

$$K = R^{-1} B^T P \tag{33}$$

and P is the solution of the continuous-time algebraic Riccati equation:

$$A^T P + PA - PBR^{-1}B^T P + Q = 0 \tag{34}$$

Naive application of equal diagonal costs in R produces unsatisfactory results, mainly because the inputs are not evenly scaled. More specifically, the force $\tilde{F}$ is on the scale of tens of Newtons, while the torque $\tilde{\tau}$ is typically less than $10Nm$. In this way, a choice of $R = \text{diag}(1,1) = \begin{bmatrix} 1 & 0 \\ 0 & 1 \end{bmatrix}$ produces very low proportional and derivative gains for the extension degree of freedom, $\tilde{l}$ and $\dot{\tilde{l}}$, that cannot be of practical use on the physical machine.

ACKNOWLEDGMENTS

This work was supported by the ARL/GDRS RCTA project, Coop. Agreement #W911NF-10-2-0016.

REFERENCES

[1] Kenneally, G., De, A., and Koditschek, D., "Design principles for a family of direct-drive legged robots," *IEEE Robotics and Automation Letters* (2016).

[2] Brown, S. and Passino, K., "Intelligent control for an acrobot," *Journal of Intelligent and Robotic Systems: Theory and Applications, 18 (3), pp. 209-248* (1997).

[3] Kwakernaak, H. and Sivan, R., [*Linear Optimal Control Systems*], Wiley-Interscience (1972 (First Edition)).

[4] Kaneko, K. e. a., ""humanoid robot hrp-2"," *IEEE Int. Conf. Robotics and Automation, p. 10831090* (2004).

[5] Kim, J.-H. and Oh, J.-H., "realization of dynamic walking for the humanoid robot platform khr-1," *Adv Robotics, 18(7):749768* (2004).

[6] Kuindersma, S., Deits, R., Fallon, M., Valenzuela, A., Dai, H., Permenter, F., Koolen, T., Marion, P., and Tedrake, R., "Optimization-based locomotion planning, estimation, and control design for the atlas humanoid robot," *Autonomous Robots, 40 (3), pp. 429-455* (2016).

[7] Playter, R. R. and Raibert, M. H., "Control of a biped somersault in 3d," *IEEE/RSJ INternational Conference on Intelligent Robots and Systems* (1992).

[8] Hereid, A., Van Why, J., Kolathaya, S., Hurst, J., Jones, M., and Ames, A., "Dynamic multi-domain bipedal walking with atrias through slip based human-inspired control," *17th International Conference on Hybrid Systems: Computation and Control* (2014).

[9] Neville, N., Buehler, M., and Sharf, I., "A bipedal running robot with one actuator per leg,"

[10] Caux, S., Mateo, E., and Zapata, R., "Balance of biped robots: Special double-inverted pendulum," *Proceedings of the IEEE International Conference on Systems, Man and Cybernetics, 4, pp. 3691-3696* (1998).

[11] Kenneally, G. and Koditschek, D. E., "Leg design for energy management in an electromechanical robot," *IEEE/RSJ International Conference on Intelligent Robots and Systems* (2015).

[12] Berkemeier, M. and Fearing, R., [*Control of a two-link robot to achieve sliding and hopping gaits*], 286–291 vol.1 (May 1992).

[13] ams AG, "As5145b datasheet," (2016).